Inorg. Chem. **2007**, *46*, 10003–10015

Inorganic Chemistry
Article

Synthesis, Reactivity, and Properties of N-Fused Porphyrin Rhenium(I) Tricarbonyl Complexes

Motoki Toganoh,[†] Shinya Ikeda,[†] and Hiroyuki Furuta*[,†,‡]

Department of Chemistry and Biochemistry, Graduate School of Engineering, Kyushu University, 744 Motooka, Nishi-ku, Fukuoka 819-0395, Japan, PRESTO, Japan Science and Technology Agency, Kawaguchi, Saitama 332-0012, Japan

Received June 20, 2007

The thermal reactions of N-fused tetraarylporphyrins or N-confused tetraarylporphyrins with $Re_2(CO)_{10}$ gave the rhenium(I) tricarbonyl complexes bearing N-fused porphyrinato ligands (**4**) in moderate to good yields. The rhenium complexes **4** are characterized by mass, IR, ^{1}H, and ^{13}C NMR spectroscopy, and the structures of tetraphenylporphynato complex **4a** and its nitro derivative **15** are determined by X-ray single crystal analysis. The rhenium complexes **4** show excellent stability against heat, light, acids, bases, and oxidants. The aromatic substitution reactions of **4** proceed without a loss of the center metal to give the nitro (**15**), formyl (**16**), benzoyl (**17**), and cyano derivatives (**19**), regioselectively. In the electrochemical measurements for **4**, one reversible oxidation wave and two reversible reduction waves are observed. Their redox potentials imply narrow HOMO–LUMO band gaps of **4** and are consistent with their electronic absorption spectra, in which the absorption edges exceed 1000 nm. Theoretical study reveals that the HOMO and LUMO of the rhenium complexes are exclusively composed of the N-fused porphyrin skeleton. Protonation of **4** takes place at the 21-position regioselectively, reflecting the high coefficient of the C21 atom in the HOMO orbital. The skeletal rearrangement reaction from N-confused porphyrin Re(I) complex (**8**) to N-fused porphyrin Re(I) complex (**4**) is suggested from the mechanistic study as well as DFT calculations.

Introduction

Porphyrin skeletons are of great importance in nature, because a number of functions such as oxygen transport, photosynthesis, electron transport, energy production, and so on, are developed by the aid of these frameworks.[1] Inspired by such multifunctionality, many organic chemists have envisioned versatile porphyrin analogues as well as porphyrin derivatives and, as a result, plenty of novel porphyrinoids have been successfully synthesized. During these studies, two important strategies, *expansion* and *confusion*, were developed and significantly contributed to the production of porphyrin variants, which have accelerated the development of coordination chemistry, materials science, and electron-transfer chemistry.[2] Recently, completely new strategy, *fusion*, was serendipitously discovered and new macrocyclic compounds have been synthesized on the basis of this strategy (Chart 1).[3,4] In these compounds, drastic changes of physical and chemical properties are sparked by *fusion*. The chemistry of *fusion* was just started, and the augmented study involving the coordination chemistry has been awaited.[5]

Among the porphyrin metal complexes, rhenium(I) tricarbonyl complexes constitute a peculiarly interesting class

* To whom correspondence should be addressed. E-mail: hfuruta@cstf.kyushu-u.ac.jp.
[†] Kyushu University.
[‡] Japan Science and Technology Agency.

(1) (a) Smith, K. M. *Porphyrins and Metalloporphyrins*; Elsevier Science: Amsterdam, The Netherlands, 1975. (b) Kadish, K. M.; Smith, K. M.; Guilard, R. *The Porphyrin Handbook*; Academic Press: San Diego, 2000.
(2) (a) Lash, T. D. *Synlett* **1999**, 279. (b) Furuta, H.; Maeda, H.; Osuka, A. *Chem. Commun.* **2002**, 1795. (c) Harvey, J. D.; Ziegler, C. J. *Coord. Chem. Rev.* **2003**, *247*, 1. (d) Sessler, J. L.; Seidel, D. *Angew. Chem., Int. Ed.* **2003**, *42*, 5134. (e) Chandrashekar, T. K.; Venkatraman, S. *Acc. Chem. Res.* **2003**, *36*, 676. (f) Ghosh, A. *Angew. Chem., Int. Ed.* **2004**, *43*, 1918. (g) Stępień, M.; Latos-Grażyński, L. *Acc. Chem. Res.* **2005**, *38*, 88. (h) Chmielewski, P. J.; Latos-Grażyński, L. *Coord. Chem. Rev.* **2005**, *249*, 2510. (i) Srinivasan, A.; Furuta, H. *Acc. Chem. Res.* **2005**, *38*, 10.
(3) (a) Furuta, H.; Ishizuka, T.; Osuka, A.; Ogawa, T. *J. Am. Chem. Soc.* **1999**, *121*, 2945. (b) Furuta, H.; Ishizuka, T.; Osuka, A.; Ogawa, T. *J. Am. Chem. Soc.* **2000**, *122*, 5748.
(4) (a) Shin, J.-Y.; Furuta, H.; Osuka, A. *Angew. Chem., Int. Ed.* **2001**, *40*, 619. (b) Maeda, H.; Osuka, A.; Furuta, H. *J. Am. Chem. Soc.* **2003**, *125*, 15690. (c) Srinivasan, A.; Ishizuka, T.; Furuta, H. *Angew. Chem., Int. Ed.* **2004**, *43*, 876.
(5) Mori, S.; Shin, J.-Y.; Shimizu, S.; Ishikawa, F.; Furuta, H.; Osuka, A. *Chem.—Eur. J.* **2005**, *11*, 2417.

10.1021/ic701208g CCC: $37.00 © 2007 American Chemical Society
Published on Web 10/18/2007

Chart 1 Examples of *confused* and *fused* Porphyrins

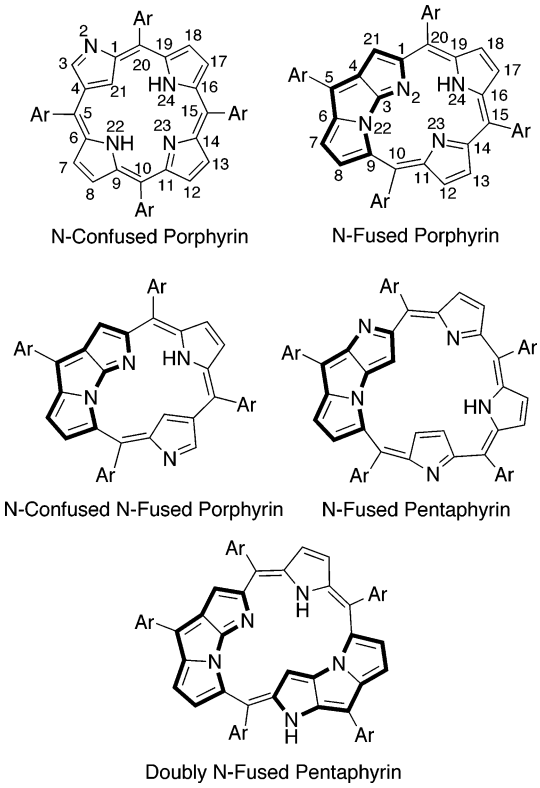

Chart 2 Structures of the Rhenium Complexes Bearing the Tripodal Porphyrinoid Ligands

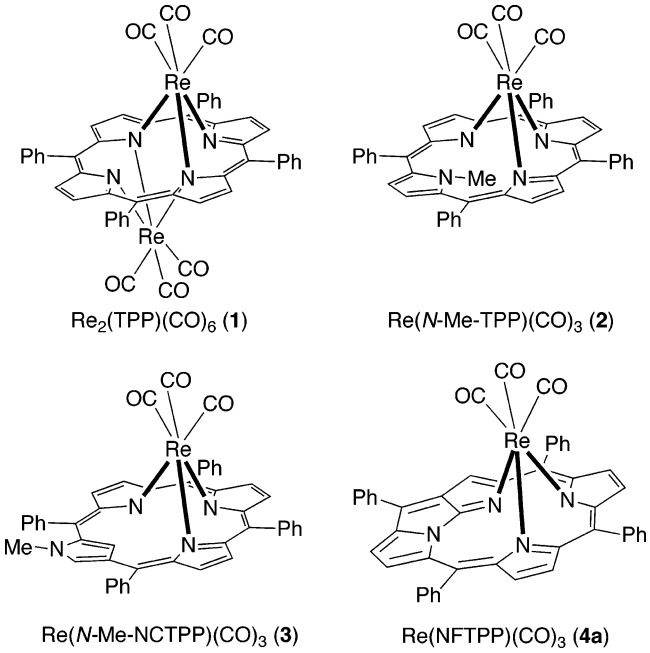

of compounds, where the three of four nitrogen atoms within the macrocyclic skeletons coordinate to the center metal (Chart 2). In 1975, Tsutsui and co-workers reported that the thermal reaction of tetraphenylporphyrin (TPP) with $Re_2(CO)_{10}$ gave a *bis*-Re(I) complex of TPP ($Re_2TPP(CO)_6$, **1**) having a tripodal structure.[6] In spite of such a unique structure and recent progress of rhenium chemistry,[7,8] further study on the rhenium tricarbonyl complexes bearing porphyrinoid ligands is not well achieved, and there remains a lot of room for investigation. Recently, we have succeeded to prepare the rhenium complexes of *N*-methyltetraphenylporphyrin ($Re(N\text{-Me}-TPP)(CO)_3$, **2**) and *N*-methyl-N-confused tetraphenylporphyrin[9] ($Re(N\text{-Me}-NCTPP)(CO)_3$, **3**).[10] The tripodal structures of **1**−**3** remind us of the structure of N-fused porphyrin, where the three coordinating nitrogen atoms are arranged in a triangle.

This time we have successfully synthesized the N-fused porphyrin rhenium complexes as the first example of N-fused porphyrin metal complexes. Thus, a thermal reaction of N-fused tetraphenylporphyrin (NFTPP) with $Re_2(CO)_{10}$ afforded a tripodal rhenium(I) tricarbonyl complex, $Re(NFTPP)(CO)_3$ (**4a**). Furthermore, we serendipitously found that a thermal reaction of N-confused tetraphenylporphyrin (NCTPP)[11] with $Re_2(CO)_{10}$ directly gave **4a** through an unexpected skeletal rearrangement from NCTPP to NFTPP.[3] In this article, full details on synthesis, reactivity, and properties of the N-fused porphyrin rhenium tricarbonyl complexes are described.[12]

Results and Discussion

Synthesis and Properties of $Re(NFTPP)(CO)_3$. When a mixture of NCTPP and $Re_2(CO)_{10}$ in 1,2-dichlorobenzene was heated at 160 °C, NCTPP was slowly consumed, and a less-polar product was detected in TLC analysis as a reddish-purple spot. Then, the mixture was further heated at 160 °C for 36 h, where the complete consumption of NCTPP was confirmed by TLC analysis. After silica gel column separation of the crude product, the less-polar compound was isolated in a pure form as a reddish-purple solid. Spectral analysis reveals that the isolated compound is not the expected rhenium(I) NCTPP complex but the rhenium(I) tricarbonyl complex bearing an N-fused tetraphenylporphynato ligand, $Re(NFTPP)(CO)_3$ (**4a**).

All of the spectral data for **4a** are fully consistent with the assigned structure. By mass spectrum analysis, the parent ion peak is observed at $m/z = 880$ (M^+) in ESI mode, and the reasonable fragment peak is detected at $m/z = 796$ ($[M-3(CO)]^+$) in MALDI mode. The ^1H NMR signals appear in the region from 7.3 to 9.3 ppm and resemble to those of the free-base NFTPP except for a loss of the singlet signal due

(6) (a) Tsutsui, M.; Ostfeld, D.; Hrung, C. P.; Conway, D. C. *J. Am. Chem. Soc.* **1971**, *93*, 2548. (b) Tsutsui, M.; Hrung, C. P.; Ostfeld, D.; Srivastava, T. S.; Cullen, D. L.; Meyer, E. F., Jr. *J. Am. Chem. Soc.* **1975**, *97*, 3952.
(7) (a) Casey, C. P. *Science* **1993**, *259*, 1552. (b) Romão, C. C.; Kühn, F. E.; Hermann, W. A. *Chem. Rev.* **1997**, *97*, 3197. (c) Kühn, F. E.; Santos, A. M.; Herrmann, W. A. *Dalton Trans.* **2005**, 2483.
(8) (a) Chen, H.; Hartwig, J. F. *Angew. Chem., Int. Ed.* **1999**, *38*, 3391. (b) Chong, D.; Nafady, A.; Costa, P. J.; Calhorda, M. J.; Geiger, W. E. *J. Am. Chem. Soc.* **2005**, *127*, 15676. (c) Kuninobu, Y.; Kawata, A.; Takai, K. *J. Am. Chem. Soc.* **2005**, *127*, 13498. (d) Lawes, D. J.; Geftakis, S.; Ball, G. E. *J. Am. Chem. Soc.* **2005**, *127*, 4134.
(9) Chmielewski, P. J.; Latos-Grażyński, L. *J. Chem. Soc., Perkin Trans. 2* **1995**, 503.
(10) Toganoh, M.; Furuta, H. *Chem. Lett.* **2005**, *34*, 1034.
(11) (a) Furuta, H.; Asano, T.; Ogawa, T. *J. Am. Chem. Soc.* **1994**, *116*, 767. (b) Chmielewski, P. J.; Latos-Grażyński, L.; Rachlewicz, K.; Glowiak, T. *Angew. Chem., Int. Ed. Engl.* **1994**, *33*, 779. (c) Morimoto, T.; Taniguchi, S.; Osuka, A.; Furuta, H. *Eur. J. Org. Chem.* **2005**, 3887.
(12) Preliminary communication: Toganoh, M.; Ishizuka, T.; Furuta, H. *Chem. Commun.* **2004**, 2464.

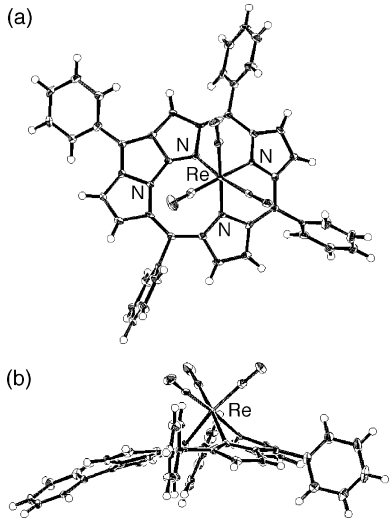

Figure 1. Crystal structure of **4a**; (a) top view, (b) side view. The solvent molecule is omitted for clarity. Thermal ellipsoids are shown at the 30% probability level.

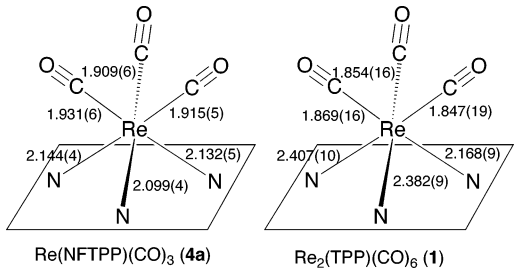

Figure 2. Bond lengths (Å) around the metal center of **4a** and **1**. The data for **1** are taken from ref 6b.

to the NH moiety. In the ^{13}C NMR spectrum, the signals due to the three CO ligands are distinctly observed at 193.24, 193.52, and 193.71 ppm, and the number of other signals is appropriate for the NFTPP substructure. The strong absorption bands due to the CO stretching vibrations are clearly observed at 1893 and 1999 cm^{-1} in the IR spectrum. These values are typical for the coordinated CO ligands.

The details on the structure of **4a** were elucidated by X-ray crystallographic analysis. Slow diffusion of hexane into a CH_2Cl_2 solution of **4a** gave violet crystals, one of which was subjected to X-ray analysis. The crystal structure of **4a** is shown in Figure 1. The three nitrogen atoms point upward, so as to coordinate to the rhenium metal, and thus the NFTPP plane has a slightly bent structure. The rhenium atom is placed above the midst of the three nitrogen atoms, and all of the Re−N bonds are in the same straight line with each CO ligand. The bond lengths around the center metals of NFTPP complex **4a** and TPP complex **1** are shown in Figure 2.[6] The Re−N bond lengths of **4a** (av 2.13 Å) are significantly shorter than those of **1** (av 2.32 Å), and the Re−CO bond lengths of **4a** (av 1.92 Å) are slightly longer than those of **1** (av 1.86 Å). These data suggest that the three coordinating nitrogen atoms of the N-fused porphyrinato ligand are arranged properly and strongly coordinate to the center metal.

Rhenium complex **4a** is extremely stable against light, heat, acids, bases, and oxidants. For example, no decomposition was observed on exposure to air and sunlight in a CH_2Cl_2 solution over a month. Thermal stability is rather noteworthy; **4a** remained unchanged after heating at 250 °C for 1 h in a sealed tube under reduced pressure (∼0.3 mmHg). Besides, in CH_2Cl_2, no decomposition was observed by treatment with excess amounts of acids (CF_3SO_3H, CF_3CO_2H, H_2SO_4), bases (pyridine, Et_3N, NaOH), and oxidant (H_2O_2) in air at ambient temperature. The stability of **4a** toward strong acids is outstanding among the porphyrinoid metal complexes, which enables **4a** to undergo the aromatic substitution reactions without a loss of the center metal (vide infra).

Scheme 1 Preparation of **4a** from NCTPP

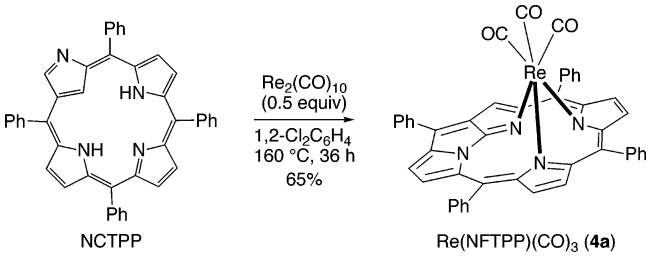

NFTPP complex **4a** was also prepared via the free-base NFTPP using the stepwise protocol reported previously (Scheme 2).[3] An abbreviation **Re** (= $Re(CO)_3$) is used to simplify the chemical structures in the schemes. Treatment of NCTPP with *N*-bromosuccinimide (NBS) gave 3,21-Br_2−NCTPP (**5**), then, the ring fusion reaction of **5** took place in pyridine spontaneously to afford 21-Br−NFTPP (**6**), and heating of **6** in pyridine gave intact NFTPP (**7**). Finally, the thermal reaction of **7** with $Re_2(CO)_{10}$ at 130 °C for 41 h gave **4a** in 77% yield (route C). Surprisingly, the reaction of **6** with $Re_2(CO)_{10}$ also gave **4a** in 63% yield (route B), indicating that $Re_2(CO)_{10}$ could be used for debromination reactions of the brominated porphyrinoid compounds. Whereas the reactions from the NFTPP derivatives proceed cleanly, they are prepared from NCTPP in multiple steps, and the total yields from NCTPP to **4a** are much lower than the direct reaction of NCTPP with $Re_2(CO)_{10}$ (route A). Thus, the direct method (route A) seems to be the most convenient and efficient for the preparation of N-fused porphyrin rhenium complexes.

Mechanistic Study. A plausible mechanism for the reaction from NCTPP to **4a** is shown in Scheme 3, which is supported by some control experiments. When NCTPP was heated at 160 °C in the absence of $Re_2(CO)_{10}$, no reaction took place. In the reaction with a catalytic amount of $Re_2(CO)_{10}$, only the starting NCTPP and NFTPP complex **4a** were observed in TLC as well as ^{1}H NMR analyses. These results suggest that the conversion from NCTPP to NFTPP requires the aid of rhenium metal. Meanwhile, when the reaction was carried out with an excess amount of $Re_2(CO)_{10}$ (0.8 equiv), essentially the same results were obtained with the case of 0.5 equiv of $Re_2(CO)_{10}$. Namely, one rhenium metal is enough for the reaction. Accordingly, a rhenium metal that assists the conversion of NCTPP to NFTPP is most likely identical with a rhenium metal that is introduced to the NFTPP molecule.

Scheme 2 Preparation of **4a** via NFTPP

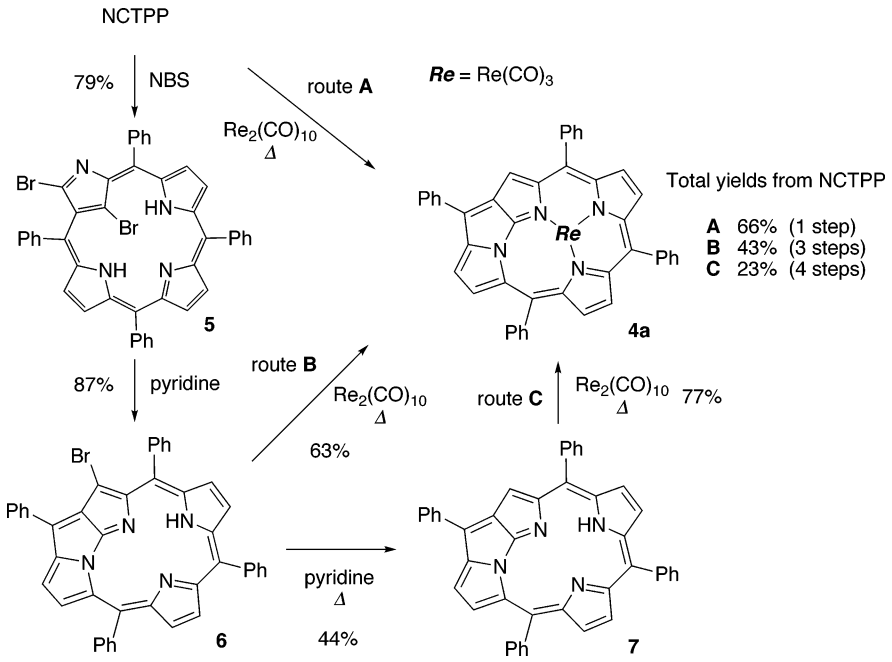

Scheme 3 Plausible Mechanism for the Reaction of NCTPP with $Re_2(CO)_{10}$[a]

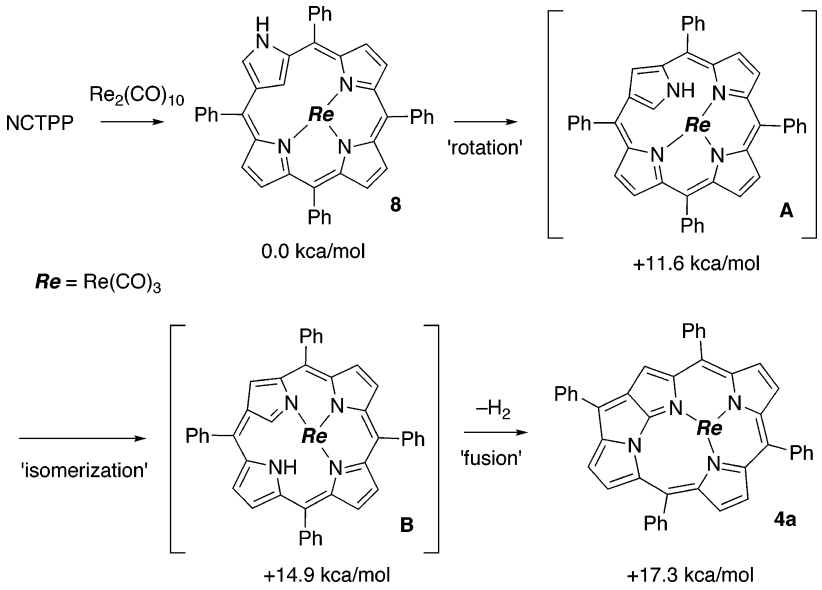

[a] The values below the structures are the calculated relative energies at the B3LYP/631LAN level. The energy for **4a** includes that for a hydrogen molecule.

On the basis of these observations as well as precedent studies,[13] the mechanism of the conversion from NCTPP to **4a** is supposed as follows. First, coordination of a rhenium metal to NCTPP through N−H bond activation occurs to give $Re(NCTPP)(CO)_3$ (**8**) in a similar manner as the reaction of *N*-Me−NCTPP with $Re_2(CO)_{10}$.[5,14] Second, the rotation of the confused pyrrole ring proceeds to give an inverted conformer of **8** (intermediate **A**). The inverted form of N-confused porphyrin is experimentally observed in the N-confused porphyrin dimer.[15] Then, migration of the rhenium atom as well as the hydrogen atom causes the production of an intermediate **B**. Trapping of the inverted form of the N-confused porphyrin by metal coordination is already reported with the NCTPP iridium complex.[16] Finally, a ring fusion reaction through a loss of the hydrogen molecule affords **4a**. To support the proposed mechanism, the relative energies for **8**, **A**, **B,** and **4a**(+H_2) were calculated at the B3LYP/631LAN level. Whereas all of the steps are theoretically endothermic, the energy differences are small enough under the thermal-reaction conditions applied here,

(13) Szterenberg, L.; Latos-Grażyński, L. *J. Porphyrins Phthalocyanines* **2001**, *5*, 474.
(14) (a) Patton, A. T.; Strouse, C. E.; Knobler, C. B.; Gladysz, J. A. *J. Am. Chem. Soc.* **1983**, *105*, 5804. (b) Toganoh, M.; Matsuo, Y.; Nakamura, E. *Angew. Chem., Int. Ed.* **2003**, *42*, 3530.
(15) Ishizuka, T.; Osuka, A.; Furuta, H. *Angew. Chem., Int. Ed.* **2004**, *43*, 5077.
(16) Toganoh, M.; Konagawa, J.; Furuta, H. *Inorg. Chem.* **2006**, *45*, 3852.

Scheme 4 Preparation of **8**

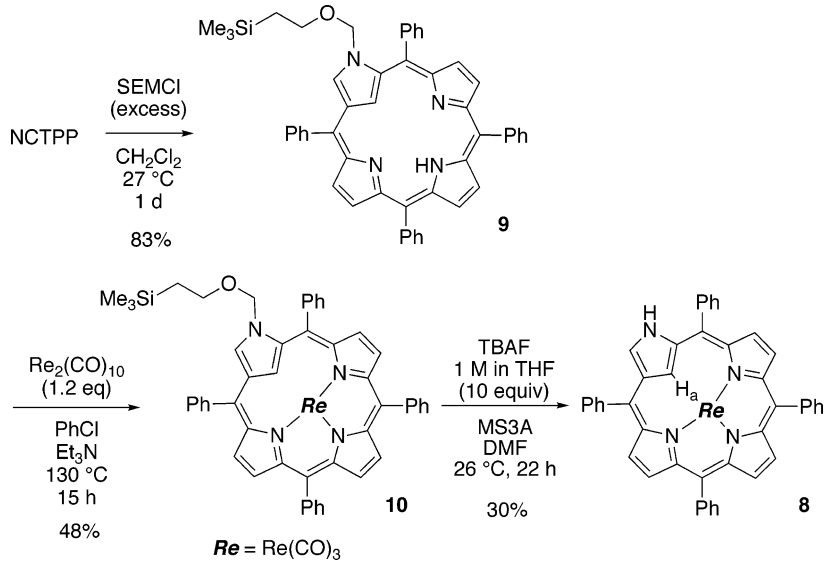

and a loss of the hydrogen molecule at the final step would be a good driving force in the whole reaction.

Furthermore, $Re(NCTPP)(CO)_3$ (**8**) was prepared through the protection/deprotection protocol to verify that **8** is a possible intermediate. Upon the treatment of NCTPP with an excess amount of 2-(trimethylsilyl)ethoxymethyl chloride (SEMCl)[17] at 27 °C for 1 d, *N*-SEM-NCTPP (**9**) was obtained in 83% yield. Whereas HCl molecules, generated through the reaction, would cause the decomposition of **9** and SEMCl, the reactions under the basic conditions (Et_3N, $NaHCO_3$, or AcONa) gave significant amounts of dialkylated products as a mixture of two isomers, and hence the best yield so far was obtained in the reaction without the bases. The thermal reaction of **9** with $Re_2(CO)_{10}$ gave Re(*N*-SEM-NCTPP)$(CO)_3$ (**10**) in 48% yield without losing the SEM group. The presence of Et_3N in this step caused a slight improvement in the isolated yield. Whereas the center metal of **10** was readily removed under the acidic conditions, deprotection without a loss of the metal was successfully achieved by treatment with TBAF in DMF in the presence of molecular sieves (MS3A), affording **8** in 30% yield. The rest of the crude product in the deprotection reaction was mainly composed of the starting compound (**10**), and it could be recovered by silica gel column separation.

8 was characterized by spectroscopic techniques. In MALDI-TOF mass analysis, the molecular ion peaks corresponding to the $[M-H]^-$ species (m/z = 881.1) are observed with an appropriate isotope pattern.[18] The strong IR absorption signals due to the CO stretching vibrations are clearly detected at 2010 and 1886 cm^{-1}. The ^1H NMR and ^{13}C NMR spectra are fully consistent with the assigned structure. For example, a broad signal due to the peripheral NH moiety of the confused pyrrole ring appears at 9.45 ppm. The signal due to the β-hydrogen atom of the confused pyrrole ring (H_a in Scheme 4), located inside of the macrocyclic core, is shown at −0.45 ppm. The ^{13}C NMR signals due to the three CO ligands are unambiguously detected at 190.36, 191.35, and 192.29 ppm.

Scheme 5 Thermal Skeletal Rearrangement from **8** to **4a**

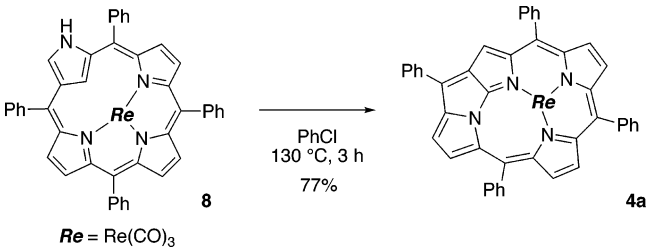

Expectedly, heating of **8** either in chlorobenzene or pyridine caused the skeletal rearrangement from NCTPP to NFTPP to give $Re(NFTPP)(CO)_3$ (**4a**) in good yields, indicating that **8** is a possible intermediate for the direct conversion from NCTPP to **4a**. For example, heating of **8** in chlorobenzene at 130 °C for 3 h afforded **4a** in 77% yield (Scheme 5). This result shows a sharp contrast with the reactivity of the NCTPP manganese complexes.[19] Heating of NCTPP with $Mn_2(CO)_{10}$ gives a dimeric NCTPP Mn(II) complex. No Mn(I) species like the rhenium case is reported. Further heating of the Mn(II) complex in pyridine causes C−H bond activation of the inner C−H moiety (corresponding to H_a of **8** in Scheme 4). A skeletal rearrangement from NCTPP to NFTPP is never observed yet in the manganese complexes. The reaction temperature required here (130 °C) is significantly lower than that for the direct reaction of NCTPP with $Re_2(CO)_{10}$ (160 °C), and it is consistent with the fact that **8** is not observed during the direct reaction.

Reactions of NCTPP Derivatives with $Re_2(CO)_{10}$. To investigate the generality of the rhenium-mediated skeletal rearrangement from N-confused porphyrins to N-fused porphyrins, a variety of N-confused tetraarylporphyrins were subjected to the reactions (Table 1). Whereas the reaction

(17) (a) Muchowski, J. M.; Solas, D. R. *J. Org. Chem.* **1984**, *49*, 203. (b) Edwards, M. P.; Doherty, A. M.; Ley, S. V.; Organ, H. M. *Tetrahedron* **1986**, *42*, 3723.

(18) Calculated relative intensities: 881(4.1), 882 (2.2), 883 (7.5), 884 (3.8), 885 (1.0). Found: 881(4.3), 882 (2.5), 883 (8.1), 884 (4.5), 885 (1.0).

(19) (a) Harvey, J. D.; Ziegler, C. J. *Chem. Commun*. **2002**, 1942. (b) Harvey, J. D.; Ziegler, C. J. *Chem. Commun*. **2003**, 2890.

Table 1. Reactions of N-Confused Tetraarylporphyrins with $Re_2(CO)_{10}$

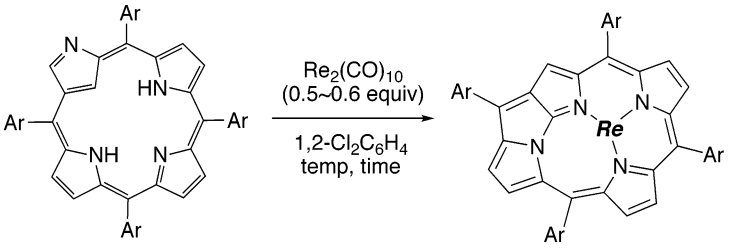

Entry	Ar	Yield (temp, time)	Entry	Ar	Yield (temp, time)
1	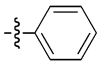	**4a**, 65% (160 °C, 36 h)	6	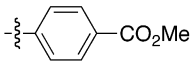	**4f**, 49% (160 °C, 3 h)
2	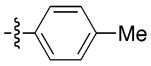	**4b**, 39% (160 °C, 7 h)	7	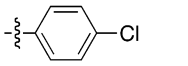	**4g**, 30% (160 °C, 15 h)
3	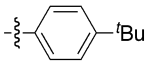	**4c**, 36% (160 °C, 17 h)	8	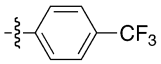	**4h**, 56% (160 °C, 14 h)
4	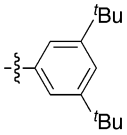	**4d**, 52% (160 °C, 20 h)	9	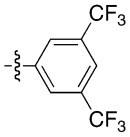	**4i**, 29% (160 °C, 21 h)
5	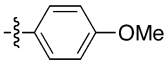	**4e**, 47% (160 °C, 12 h)	10	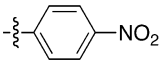	**4j**, 28% (130 °C, 18 h)

conditions were not optimized, the desired rhenium complexes were successfully obtained in all of the cases. The alkyl groups, including sterically demanding ones, do not disturb the reactions (Entries 2−4). Introduction of the electron-donating group (Entry 5) and electron-withdrawing groups (Entries 6−10) onto the *meso*-aryl positions of N-confused porphyrin does not affect the reaction. However, the yield decreases in the presence of strong electron-withdrawing groups. It is noteworthy that many of the functional groups, such as ether, ester, and nitro groups, are tolerant to the reaction conditions. Because N-confused tetraarylporphyrins are prepared in one step from pyrrole and arylaldehyde,[11,20] a wide variety of N-fused porphyrin rhenium(I) tricarbonyl complexes could be prepared easily in two steps from commercially available reagents.

Next, the reactions of 21-substituted NCTPP derivatives were attempted to obtain the 21-substituted **4a** derivatives (Scheme 6). When 21-NO_2−NCTPP (**11**)[21] was reacted with $Re_2(CO)_{10}$, the nitro group was completely removed to give **4a** in 39% yield. In the case of 21-Br−NCTPP (**12**),[3] the thermal stability of **12** was not enough for this reaction, and no rhenium complex was obtained at all. Meanwhile, 21-Cl−NCTPP (**13**) could tolerate the reaction conditions to afford a mixture of Re(21-Cl−NFTPP)$(CO)_3$ (**14**, 19% yield) and **4a** (10% yield). Though **14** was obtained as the major product, the reaction seems to be impractical because the separation of **4a** and **14** by ordinary column chromatography is quite tedious.

Scheme 6 Reactions of 21-substituted NCTPP Derivatives with $Re_2(CO)_{10}$

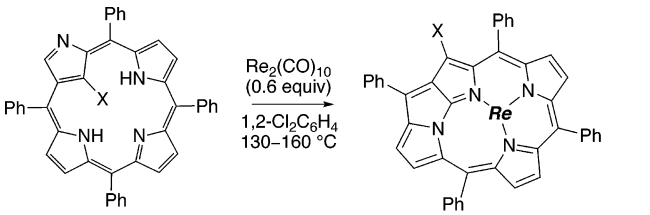

X = NO_2	**11**	Not detected.	(**4a**: 39%)
X = Br	**12**	Not detected.	
X = Cl	**13**	**14**: 19%	(**4a**: 10%)

Chemical Functionalization of 4a. Because the reactions of 21-substituted NCTPP derivatives with $Re_2(CO)_{10}$ were not effective, chemical modification of **4a** was achieved to prepare the functionalized N-fused porphyrin rhenium complexes. First, nitration of **4a** was examined under the common reaction conditions ($NaNO_2$/HCl). The nitration reaction proceeded efficiently and instantly to afford Re(21-NO_2−NFTPP)$(CO)_3$ (**15**) in 95% yield. The reaction was completely regioselective, and **15** was obtained exclusively. The structure of **15** was confirmed by X-ray crystallographic analysis (Figure 3).

(20) (a) Geier, G. R., III; Haynes, D. M.; Lindsey, J. S. *Org. Lett.* **1999**, *1*, 1455. (b) Shaw, J. L.; Garrison, S. A.; Aleman, E. A.; Ziegler, C. J.; Modarelli, D. A. *J. Org. Chem.* **2004**, *69*, 7423.

(21) Ishikawa, Y.; Yoshida, I.; Akaiwa, K.; Koguchi, E.; Sasaki, T.; Furuta, H. *Chem. Lett.* **1997**, *26*, 453.

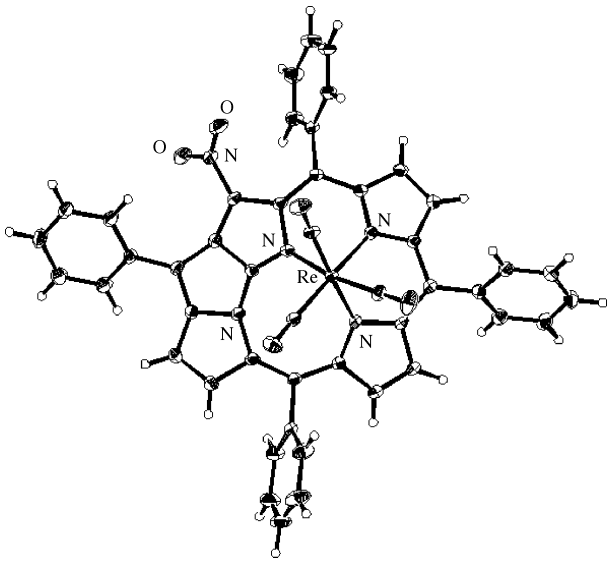

Figure 3. Crystal structure of **15**. The solvent molecule is omitted for clarity. Thermal ellipsoids are shown at the 30% probability level.

Scheme 7 Nitration of **4a**

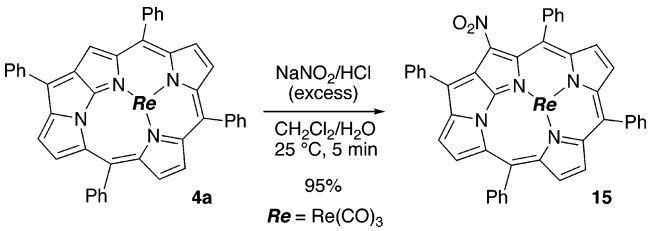

Other aromatic substitution reactions on **4a** invariably occurred at the 21 position to give the functionalized N-fused porphyrin rhenium complexes (Scheme 8). The Vilsmeier−Haak formylation of **4a** with $POCl_3$/DMF gave Re(21-CHO−NFTPP)$(CO)_3$ (**16**) in 67% yield and the Friedel−Crafts acylation with PhCOCl/$AlCl_3$ gave Re(21-PhCO−NFTPP)$(CO)_3$ (**17**) in 32% yield. Bromination of **4a** with NBS afforded Re(21-Br−NFTPP)$(CO)_3$ (**18**) in a good yield (∼80%). Whereas **18** was produced as the major product, isolation in a pure form was so far troublesome due to the difficulty in the chromatographic separation of a mixture of **18**, **4a**, and a dibrominated product.[22] Subsequent treatment of this mixture with CuCN afforded Re(21-CN−NFTPP)$(CO)_3$ (**19**) in 53% yield from **4a** (2 steps).

UV−Vis spectrum. The UV−vis spectra of **4a** and the intact NFTPP (**7**) in CH_2Cl_2 are shown in Figure 4, and the numerical data of all of the complexes studied are listed in Table 2. Despite the curved structure, the UV−vis spectrum of **4a** is quite similar to that of **7** having a planar structure. In the absorption spectrum of **4a**, the two bands (358 and 496 nm) appear in the Soret region, and the Q-type bands are shown at 859 and 951 nm. The absorption edge of **4a** reaches to 1000 nm, indicating that the rhenium coordination does not disrupt the aromatic character of the NFTPP skeleton. Substitution effect was examined using **4a** as a standard. The longest λ_{max} values are summarized in Figure

(22) The dibrominated compound was obtained as a single isomer.

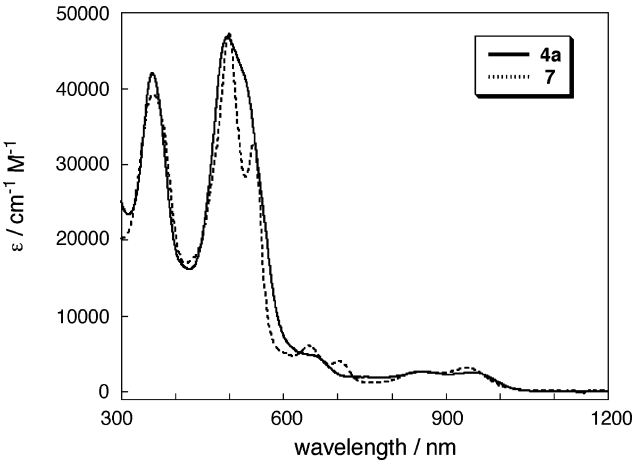

Figure 4. Absorption spectra of **4a** and **7** in CH_2Cl_2.

Scheme 8 Regioselective Aromatic Substitution Reactions of **4a**

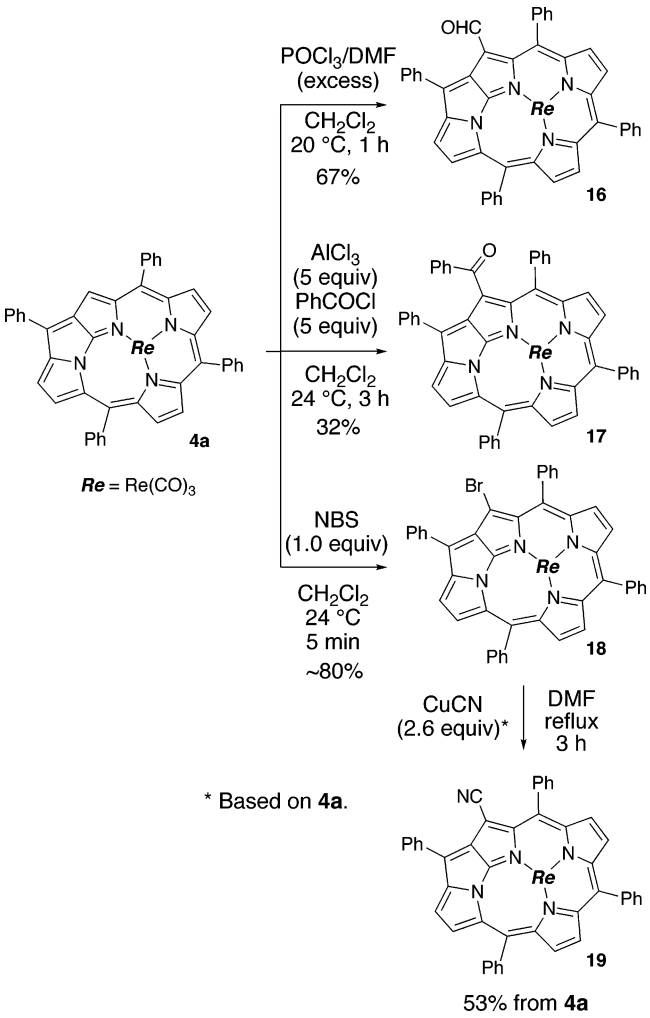

5. Introduction of the functional groups onto the *meso*-aryl positions causes modest changes in the absorption wavelengths. Small red shifts are induced by the electron-donating groups (Entry 2−5), on the other hand, small blue shifts are induced by the electron-withdrawing groups (Entry 6−10). Meanwhile, substitution at the 21 position results in a significant change in the absorption spectra because it could directly affect the [18]annulenic substructure (bold lines).

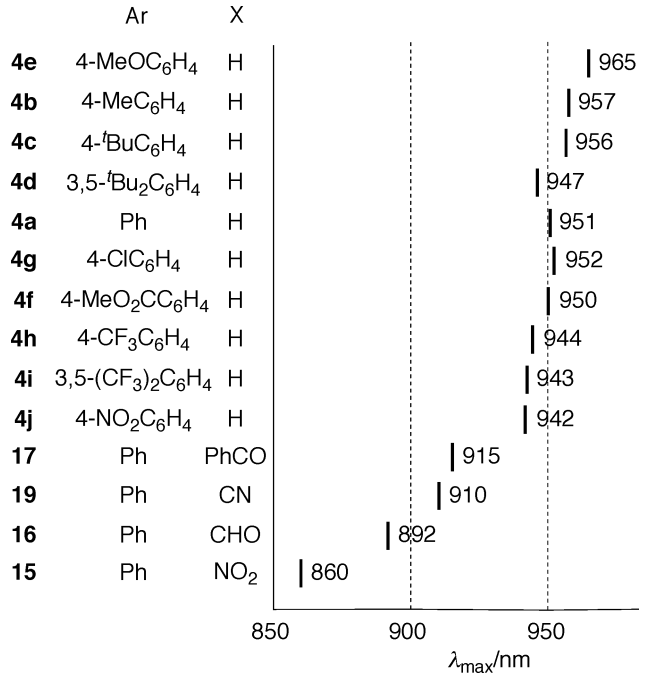

Figure 5. The longest λ_{max} values for the N-fused porphyrin rhenium complexes in CH_2Cl_2.

Table 2. Electronic Absorption Spectral Date for the N-Fused Porphyrin Rhenium Complexes in CH_2Cl_2

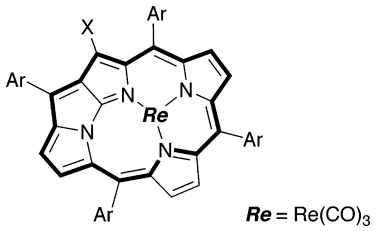

entry		Ar	X	λ_{max} (nm)				
1	**4a**	Ph	H	358	496		859	951
2	**4b**	4-MeC_6H_4	H	368	502		859	957
3	**4c**	4-$^tBuC_6H_4$	H	372	504		859	956
4	**4d**	3,5-$^tBu_2C_6H_3$	H	373	503		855	947
5	**4e**	4-$MeOC_6H_4$	H	389	510		870	965
6	**4f**	4-$MeO_2CC_6H_4$	H	353	499		854	950
7	**4g**	4-ClC_6H_4	H	362	497		854	952
8	**4h**	4-$CF_3C_6H_4$	H	353	494		847	944
9	**4i**	3,5-$(CF_3)_2C_6H_3$	H	351	494		847	943
10	**4j**	4-$NO_2C_6H_4$	H	351	507	511	845	942
11	**15**	Ph	NO_2	360	539		781	860
12	**16**	Ph	CHO	353	507	533	801	892
13	**17**	Ph	PhCO	358	500	533	842	915
14	**19**	Ph	CN	361	502		770	910

Large blue shifts are caused by the introduction of the electron-withdrawing groups at the 21 position (Entry 11−14).

Electrochemical Measurement. Cyclic voltammetry measurements on the N-fused porphyrin rhenium complexes revealed that they are robust under the electrochemical conditions, allowing one reversible one-electron oxidation as well as two reversible one-electron reductions. Further reversible oxidation or reduction was observed for **4e** or **4f**, respectively. Cyclic voltammograms of **4a** and **4e** are shown in Figure 6, and other electrochemical data are summarized in Table 3. As compared to **4a** (Entry 1), the oxidation

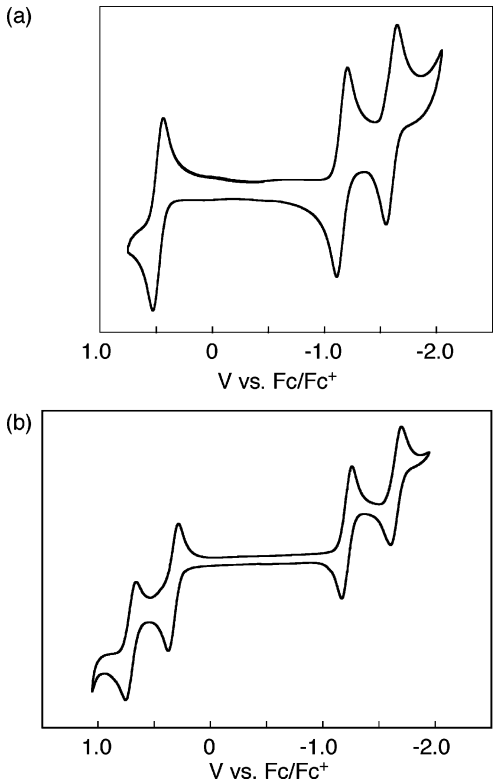

Figure 6. Cyclic voltammogram of (a) **4a** and (b) **4e** in CH_2Cl_2.

Table 3. Formal Potentials (V vs Fc/Fc^+) in CH_2Cl_2 Containing 0.1 M $^nBu_4NPF_6$

entry		Ar	X	E_{Ox1}	E_{Red1}	E_{Red2}	$E_{Ox1}-E_{Red1}$
1	**4a**	Ph	H	0.47	−1.21	−1.67	1.69
2	**4b**	4-MeC_6H_4	H	0.36	−1.26	−1.70	1.62
3	**4c**	4-$^tBuC_6H_4$	H	0.35	−1.28	−1.70	1.63
4	**4d**	3,5-$^tBu_2C_6H_3$	H	0.33	−1.31	−1.73	1.64
5	**4e**	4-$MeOC_6H_4$	H	0.33	−1.21	−1.65	1.54
6	**4f**	4-$MeO_2CC_6H_4$	H	0.56	−1.08	−1.51	1.64
7	**4g**	4-ClC_6H_4	H	0.50	−1.15	−1.60	1.65
8	**4h**	4-$CF_3C_6H_4$	H	0.61	−1.08	−1.55	1.69
9	**4i**	3,5-$(CF_3)_2C_6H_3$	H	0.75	−0.91	−1.41	1.66
10	**4j**	4-$NO_2C_6H_4$	H	0.65	−0.95	−1.30	1.60
11	**15**	Ph	NO_2	0.71	−0.95	−1.34	1.66
12	**16**	Ph	CHO	0.60	−1.06	−1.46	1.66
13	**17**	Ph	PhCO	0.50	−1.15	−1.59	1.65
14	**19**	Ph	CN	0.69	−0.99	−1.43	1.68

potentials are reasonably more negative in the presence of the electron-donating groups (Entry 2−5) and more positive in the presence of the electron-withdrawing groups (Entry 6−14). A similar trend is appropriately seen for the first and the second reduction potentials. Nevertheless, no significant differences are observed in the values of $E_{Ox1}-E_{Red1}$, which correlate with the HOMO−LUMO band gaps. Because the oxidation potentials and reduction potentials are similar to those for the parent NFTPP derivatives, both oxidations and reductions would not occur at the center metal but at the NFP skeletons.

Protonation. Interestingly, the addition of strong acids to a CH_2Cl_2 solution of **4a** causes regioselective protonation, in sharp contrast with **2** and **3**, where demetallation of the coordinated metal occurs immediately.[23] When an excess

(23) While details were not clear, treatment with CH_3SO_3H or CF_3SO_3H caused further protonation of **4a**.

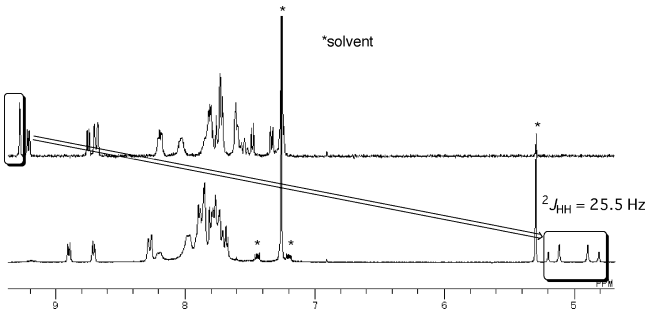

Figure 7. ^{1}H NMR spectra of **4a** (top) and **4a**+TFA (bottom) in $CDCl_3$. The boxes indicate the signals due to the protons at the 21 position.

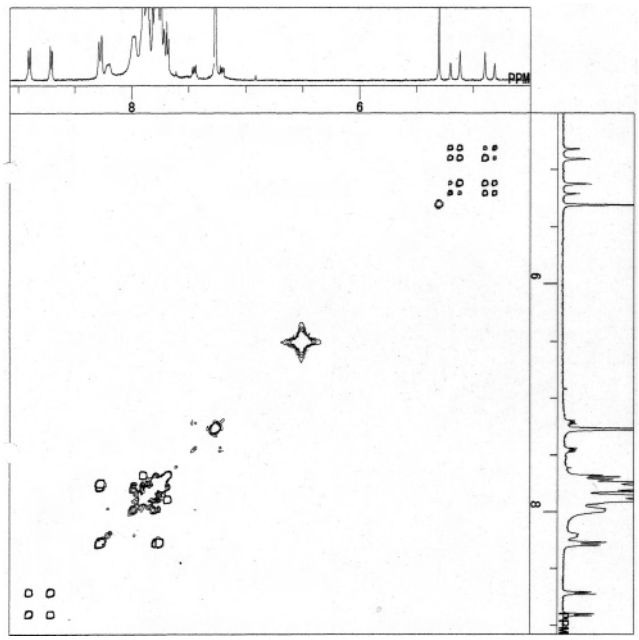

Figure 8. ^{1}H−^{1}H COSY spectrum of **4a**+TFA in $CDCl_3$.

amount of trifluoroacetic acid (TFA) was added to a CH_2Cl_2 solution of **4a**, the color of the solution changed from purple-red to brown. Subsequent treatment with Et_3N caused regeneration of the purple-red color. The ^{1}H NMR spectra of **4a** and **4a**+TFA in $CDCl_3$ are shown in Figure 7. In the ^{1}H NMR spectrum of **4a**, the singlet signal assignable to the proton at the 21 position appears at 9.28 ppm. In the presence of TFA, no singlet signal is observed around 9.28 ppm and, in turn, the two-doublet signals, which are coupled to each other in $^2J_{HH}$ = 25.5 Hz, appear at 4.85 and 5.16 ppm. The correlation is confirmed by the ^{1}H−^{1}H COSY spectrum of **4a**+TFA (Figure 8). The signal change in the ^{1}H NMR spectra suggests that the protonation occurs at the 21 position by the addition of TFA to **4a**. All of the other signals for both **4a** and **4a**+TFA are similarly observed in the aromatic proton region, indicating that the aromatic character is not lost by protonation. In fact, even after protonation at the 21 position, new [18]annulenic substructures are describable, as shown in Chart 3. Retention of the aromatic character in the protonated **4a** is also supported by the absorption spectra (Figure 9). Whereas a large blue shift at 40 nm is observed by the addition of TFA, the Soret-like band is still clearly seen in the absorption spectrum of **4a**+TFA. Hence, the protonation/deprotonation cycle is

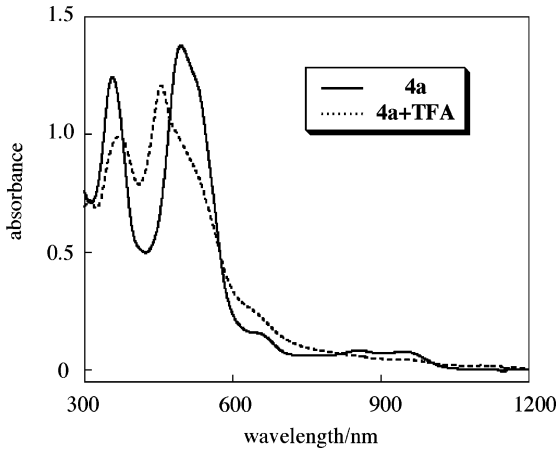

Figure 9. Absorption spectra of **4a** and **4a**+TFA.

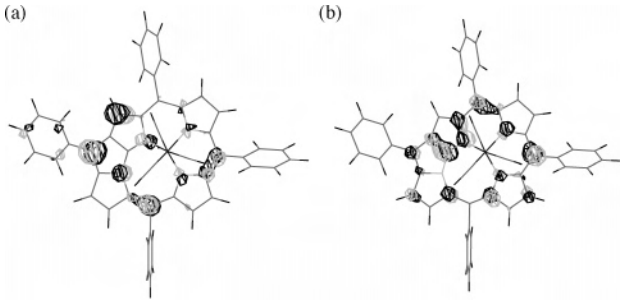

Figure 10. Kohn−Sham orbitals of **4a**; (a) HOMO, (b) LUMO.

reversible; the complex would be applicable to switching molecular devices through the change of [18]annulenic circuits. Note that protonation of the free-base NFTPP (**7**) with excess amounts of TFA occurs only at the inner-nitrogen atoms, and no protonation occurs at the 21 position, which is confirmed by ^{1}H NMR analysis.[24]

Molecular Orbitals. The Kohn−Sham orbitals of **4a** calculated at the B3LYP/631LAN level are shown in Figure 10. In the HOMO of **4a**, a large coefficient is observed at the 21 position, and it is consistent with the reactivity of **4a** shown above. In contrast, the LUMO of **4a** covers a broad range of the NFTPP skeleton. No contribution from the rhenium metal is observed for both the HOMO and the LUMO, suggesting that the first electrochemical oxidation as well as the reduction occurs at the NFTPP moiety.

Conclusion

In conclusion, a wide variety of N-fused tetraarylporphyrin rhenium(I) tricarbonyl complexes were prepared, and their optical and electrochemical properties and reactivity were investigated. The N-fused porphyrin rhenium complexes can be easily prepared from N-confused tetraarylporphyrins and $Re_2(CO)_{10}$ via the ring rearrangement and exhibit excellent stability against many harsh physical as well as chemical conditions, allowing a wide range of structural and electronic modifications. Particularly, a variety of aromatic substitution reactions proceed at the 21 position, regioselectively, without a loss of the center metal. Such features would enable

(24) Further protonation was not observed, even in the presence of excess amounts of TFA.

Chart 3 Description of [18]annuleic Circuits for **4a**+TFA

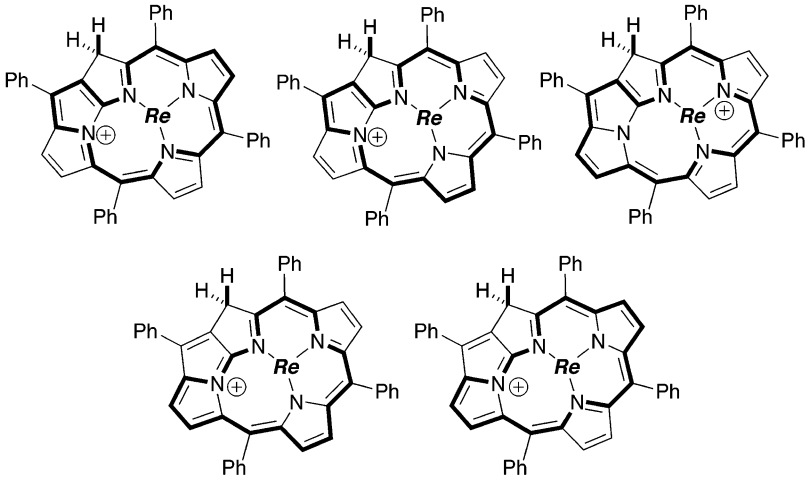

N-fused porphyrin rhenium complexes to be utilized in the field of catalyst and materials science.[7,8,25] Furthermore, it is highly probable that the N-fused tetraarylporphyrins could serve as coordination ligands for metals other than rhenium to afford novel metal complexes that exhibit unusual properties different from porphyrin complexes. Further study on the N-fused porphyrin metal complexes is now underway.

Experimental Section

General. Commercially available solvents and reagents were used without further purification unless otherwise mentioned. NBS was recrystallized from hot water. THF was distilled over benzophenone ketyl. N-confused porphyrins were synthesized according to the reported procedure.[20] Thin-layer chromatography was carried out on aluminum sheets coated with silica gel 60 (Merck 5554). Preparative purifications were performed by flash column chromatography (KANTO Silica Gel 60 N, spherical, neutral, 40−50 μm) or gravity column chromatography (KANTO Silica Gel 60 N, spherical, neutral, 63−210 μm). The ^{1}H NMR or ^{13}C NMR spectra were recorded on a JNM-AI SERIES FT-NMR spectrometer (JEOL) at 300 or 75 MHz, respectively. Proton chemical shifts were reported relative to the residual proton of the deuterated solvent (7.26 ppm for $CHCl_3$). Carbon chemical shifts were reported relative to $CDCl_3$ at 77.00 ppm. UV−vis absorption spectra were recorded on a UV-3150PC spectrometer (Shimadzu). Mass spectra were recorded on a Bruker Daltonics autoflex MALDI-TOF MS spectrometer. Cyclic voltammetric measurements were performed on a CH Instrument Model 620B (ALS) equipped with a Pt electrode. IR absorption spectra were recorded on a Spectrum One (PerkinElmer).

Reactions of N-Confused Tetraarylporphyrins with $Re_2(CO)_{10}$. Preparation of $Re(NFTPP)(CO)_3$ (4a) (Typical Procedure). A solution of NCTPP (65.3 mg, 104 μmol, 1.0 equiv) and $Re_2(CO)_{10}$ (37.1 mg, 56.9 μmol, 0.54 equiv) in 1,2-dichlorobenzene (20.0 mL) was degassed under reduced pressure (∼0.3 mmHg) at 0 °C. The resulting mixture was heated at 160 °C for 36 h under argon atmosphere. After cooling, 1,2-dichlorobenzene was removed under reduced pressure, and the residue was purified by silica gel column chromatography (eluent: CH_2Cl_2/hexane = 1:1). The first violet fraction collected was concentrated to dryness to give **4a** in 65% yield (61.0 mg, 69.1 μmol). IR (powder, cm^{-1}) 1999 (CO), 1893 (CO); ^{1}H NMR ($CDCl_3$, 300 MHz) δ ∼7.25 (1H, overlapped with a signal due to $CHCl_3$), 7.34 (d, J = 5.2 Hz, 1H), 7.49 (d, J = 4.6 Hz, 1H), 7.52−7.63 (m, 4H), 7.71−7.84 (m, 11H), 8.00−8.08 (m, 2H), 8.18−8.22 (m, 2H), 8.69 (dd, J = 0.9, 8.2 Hz, 2H), 8.75 (d, J = 5.2 Hz, 1H), 9.21 (d, J = 5.2 Hz, 1H), 9.28 (s, 1H); ^{13}C NMR ($CDCl_3$, 75 MHz) δ 111.87, 112.31, 119.47, 121.08, 123.61, 126.05, 127.46, 127.49, 128.21, 128.37, 128.49, 128.88, 129.35, 129.36, 129.82, 131.29, 131.70, 132.32, 133.01, 134.92, 136.72, 137.47, 137.75, 138.20, 140.16, 142.86, 144.92, 149.70, 153.64, 153.80, 153.99, 157.43, 163.51, 193.24, 193.52, 193.71; MS (ESI, positive) 880.1 (M^+); MS (MALDI, positive) 796.2 ([M−3(CO)]$^+$); Anal. Calcd for **4a**: C, 64.01; H, 3.09; N, 6.35. Found: C, 63.78; H, 3.20; N, 6.25; UV−vis (CH_2Cl_2, λ_{max}/nm (ϵ)) 358 (42 000), 496 (46 800), 863 (2650), 950 (2550); R_f = 0.61 (silicagel 60, CH_2Cl_2/hexane = 1:1).

Reactions of other N-confused tetraarylporphyrins followed the typical procedure.

Preparation of 4b (Tolyl). Reaction temperature: 160 °C, reaction time: 6.5 h, 39% yield. IR (powder, cm^{-1}) 2001 (CO), 1902 (CO), 1883 (CO); ^{1}H NMR ($CDCl_3$, 300 MHz) δ 2.56 (s, 3H), 2.57 (s, 3H), 2.67 (s, 3H), 2.68 (s, 3H), 7.24 (d, J = 4.6 Hz, 1H), 7.36 (d, J = 4.9 Hz, 1H), 7.41 (d, J = 7.9 Hz, 2H), 7.48 (d, J = 4.6 Hz, 1H), 7.52 (d, J = 7.9 Hz, 2H), 7.57 (d, J = 7.9 Hz, 2H), 7.63 (d, J = 7.9 Hz, 2H), 7.75 (d, J = 7.6 Hz, 2H), 7.77 (d, J = 4.9 Hz, 1H), 7.91 (d, J = 7.6 Hz, 2H), 8.11 (d, J = 7.9 Hz, 2H), 8.69 (d, J = 7.9 Hz, 2H), 8.75 (d, J = 5.2 Hz, 1H), 9.17 (d, J = 5.2 Hz, 1H), 9.30 (s, 1H); ^{13}C NMR ($CDCl_3$, 75 MHz) δ 21.40, 21.54, 21.55, 21.61, 111.78, 112.46, 119.22, 120.91, 123.50, 126.05, 127.20, 128.12, 128.23, 128.80, 129.21, 129.23, 130.54, 131.44, 131.65, 132.19, 132.33, 133.04, 135.00, 135.42, 136.51, 137.32, 137.86, 138.24, 138.52, 139.40, 140.27, 142.21, 142.66, 149.52, 153.68, 153.71, 153.97, 157.56, 163.71, 193.36, 193.64, 193.79; MS (MALDI, positive) 852.3 ([M−3(CO)]$^+$); Anal. Calcd for **4b·0.7CH_2Cl_2**: C, 62.25; H, 3.68; N, 5.62. Found: C, 62.29; H, 3.87; N, 5.99; UV−vis (CH_2Cl_2, λ_{max}/nm) 368, 502, 859, 957.

Preparation of 4c (4-*tert*-Butylphenyl). Reaction temperature: 160 °C, reaction time: 17 h, 36% yield. IR (powder, cm^{-1}) 2004 (CO), 1893 (CO); ^{1}H NMR ($CDCl_3$, 300 MHz) δ 1.52 (s, 9H), 1.53 (s, 9H), 1.61 (s, 9H), 1.63 (s, 9H), 7.34 (d, J = 4.5 Hz, 1H), 7.39 (d, J = 4.9 Hz, 1H), 7.55 (d, J = 4.5 Hz, 1H), 7.66 (d, J = 8.6 Hz, 2H), 7.76 (d, J = 8.6 Hz, 2H), 7.83−7.90 (m, 7H), 8.01 (d, J = 8.2 Hz, 2H), 8.23 (d, J = 8.2 Hz, 2H), 8.70 (d, J = 8.2 Hz, 2H), 8.84 (d, J = 5.2 Hz, 1H), 9.23 (d, J = 5.2 Hz, 1H), 9.40 (s, 1H); ^{13}C NMR ($CDCl_3$, 75 MHz) δ 31.34, 31.47, 31.54, 31.62, 34.80, 34.91, 34.94, 35.04, 111.98, 112.18, 119.30, 120.86, 123.59,

(25) Toganoh, M.; Ikeda, S.; Furuta, H. *Chem. Commun.* **2005**, 4589.

124.30, 124.45, 125.49, 126.19, 126.81, 127.27, 128.96, 129.14, 131.50, 131.61, 132.27, 132.33, 132.99, 134.95, 135.36, 136.61, 137.46, 140.33, 142.10, 142.73, 149.47, 151.07, 151.34, 151.61, 152.49, 153.50, 153.66, 153.97, 157.72, 163.80, 193.36, 193.65, 193.82; MS (MALDI, positive) 1020.5 ([M-3(CO)]$^+$); Anal. Calcd for **4c·0.3CH$_2$Cl$_2$**: C, 67.17; H, 5.31; N, 4.95. Found: C, 67.09; H, 5.16; N, 4.67; UV−vis (CH$_2$Cl$_2$, λ_{max}/nm) 372, 504, 859, 956.

Preparation of 4d ((3,5-di-*tert*-Butyl)Phenyl). Reaction temperature: 160 °C, reaction time: 20 h, 52% yield. IR (powder, cm^{-1}) 2004 (CO), 1895 (CO); ^{1}H NMR (CDCl$_3$, 300 MHz) δ 1.53 (s, 36H), 1.56 (s, 36H), 7.20 (d, J = 4.5 Hz, 1H), 7.26 (s, 1H), 7.36 (d, J = 4.8 Hz, 1H), 7.44 (d, J = 4.5 Hz, 1H), 7.61 (m, 3H), 7.73 (m, 1H), 7.78. (d, J = 4.8 Hz, 1H), 7.81 (m, 1H), 7.86 (br, s, 2H), 8.14 (d, J = 1.8 Hz, 2H), 8.57 (d, J = 2.1 Hz, 2H), 8.69 (d, J = 5.1 Hz, 1H), 9.13 (d, J = 5.1 Hz, 1H), 9.35 (s, 1H); ^{13}C NMR (CDCl$_3$, 75 MHz) δ 31.58, 31.67, 31.71, 34.95, 35.03, 35.17, 35.22, 111.96, 113.01, 120.43, 120.90, 121.53, 121.88, 122.58, 123.27, 123.84, 126.48, 127.31, 127.49, 128.01, 129.02, 131.60, 131.73, 134.49, 136.71, 137.19, 137.53, 138.65, 141.61, 142.97, 144.25, 149.26, 149.64, 150.87, 152.29, 153.43, 153.55, 154.15, 158.00, 163.83, 193.61, 193.79, 193.85; MS (MALDI) m/z = 1244.6 ([M−3(CO)]$^+$), 1272.6 ([M−2(CO)]$^+$), 1328.6 ([M]$^+$); UV−vis (CH$_2$Cl$_2$, λ_{max}/nm) 373, 503, 855, 947.

Preparation of 4e (4-Methoxyphenyl). Reaction temperature: 160 °C, reaction time: 12 h, 47% yield. IR (powder, cm^{-1}) 2000 (CO), 1887 (CO), 1880 (CO); ^{1}H NMR (CDCl$_3$, 300 MHz) δ 3.98 (s, 3H), 4.00 (s, 3H), 4.07 (s, 3H), 4.08 (s, 3H), 7.14 (d, J = 8.4 Hz, 2H), 7.22.-7.36 (m, 8H, overlapped with a peak due to CHCl$_3$), 7.47 (d, J = 4.8 Hz, 1H), 7.79 (m, 3H), 7.92 (m, 2H), 8.16 (d, J = 8.4 Hz, 2H), 8.66 (d, J = 8.4 Hz, 2H), 8.74 (d, J = 4.8 Hz, 1H), 9.15 (d, J = 4.8 Hz, 1H), 9.28 (s, 1H); ^{13}C NMR (CDCl$_3$, 75 MHz) δ 53.41, 55.47, 55.57, 55.61, 111.55, 112.69, 112.81, 113.08, 114.07, 115.44, 118.49, 120.87, 123.48, 126.19, 126.80, 127.51, 127.80, 128.77, 130.33, 130.65, 130.77, 131.70, 133.74, 134.21, 134.37, 136.26, 136.60, 137.72, 139.99, 142.29, 149.35, 153.70, 153.86, 154.02, 157.63, 159.49, 159.94, 160.03, 160.80, 164.012, 193.37, 193.65, 193.82; MS (MALDI, positive) m/z = 916.6 ([M−3CO]$^+$), 1000.5 ([M]$^+$); Anal. Calcd for **4e**: C, 61.13; H, 3.52; N, 5.59. Found: C, 61.10; H. 3.50; N, 5.67; UV−vis (CH$_2$Cl$_2$, λ_{max}/nm) 338, 389, 511, 870, 965.

Preparation of 4f (4-Methoxycarbonylphenyl). Reaction temperature: 160 °C, reaction time: 3 h, 49% yield. IR (powder, cm^{-1}) 2003 (CO), 1923 (CO), 1908 (CO), 1885 (CO), 1724 (COOMe); ^{1}H NMR (CDCl$_3$, 300 MHz) δ 4.04 (s, 6H), 4.12 (s, 6H), 7.28 (d, J = 4.5 Hz, 1H), 7.33 (d, J = 4.8 Hz, 1H), 7.51 (d, J = 4.5 Hz, 1H), 7.71 (d, J = 4.8 Hz, 1H), 7.94 (m, 2H), 8.14. (m, 2H), 8.30 (m, 4H), 8.43 (d, J = 8.4 Hz, 4H), 8.52 (d, J = 7.2 Hz, 2H), 8.76 (d, J = 8.4 Hz, 2H), 8.77 (d, J = 5.4 Hz, 1H), 9.29 (s, 1H), 9.31 (d, J = 5.4 Hz, 1H); ^{13}C NMR (CDCl$_3$, 75 MHz) δ 52.39, 52.44, 52.52, 52.57, 111.34, 111.81, 119.30, 121.51, 123.94, 126.19, 127.74, 128.76, 128.84, 129.00, 129.51, 129.74, 130.27, 130.31, 130.68, 131.04, 131.21, 131.83, 132.28, 132.94, 136.74, 136.95, 138.90, 139.07, 141.88, 142.48, 143.40, 148.97, 149.74, 153.43, 153.72, 153.85, 157.16, 162.53, 166.68, 166.80, 166.89, 192.68, 193.05, 193.38; MS (MALDI, positive) m/z = 1027.5 ([M−3CO]$^+$); UV−vis (CH$_2$Cl$_2$, λ_{max}/nm) 353, 499, 854, 950.

Preparation of 4g (4-Chlorophenyl). Reaction temperature: 160 °C, reaction time: 15 h, 30% yield. IR (powder, cm^{-1}) 2003 (CO), 1905 (CO), 1887 (CO); ^{1}H NMR (CDCl$_3$, 300 MHz) δ 7.27 (d, J = 4.3 Hz, 1H), 7.37 (d, J = 4.9 Hz, 1H), 7.52 (d, J = 4.3 Hz, 1H), 7.66 (d, J = 8.6 Hz, 2H), 7.70−7.83 (m, 9H), 7.96 (d, J = 7.9 Hz, 2H), 8.12 (d, J = 7.9 Hz, 2H), 8.61 (d, J = 8.5 Hz, 2H), 8.76 (d, J = 5.5 Hz, 1H), 9.20 (d, J = 5.5 Hz, 1H), 9.22 (s, 1H); ^{13}C NMR (CDCl$_3$, 75 MHz) δ 111.41, 111.61, 118.38, 121.23, 123.71, 126.19, 127.32, 127.87, 127.93, 128.74, 128.94, 130.19, 130.42, 131.16, 131.83, 133.19, 133.41, 134.07, 134.65, 134,72, 135.12, 135.94, 135.99, 136.13, 136.44, 136.69, 138.87, 142.87, 143.11, 149.61, 153.72, 153.82, 153.94, 157.20, 163.13, 192.80, 193.17, 193.46; MS (MALDI, positive) 932.2 ([M−3(CO)]$^+$); UV−vis (CH$_2$Cl$_2$, λ_{max}/nm) 362, 497, 854, 952.

Preparation of 4h ((4-Trifluoromethyl)Phenyl). Reaction temperature: 160 °C, reaction time: 21 h, 53% yield. IR (powder, cm^{-1}) 2009 (CO), 1949 (CO), 1925 (CO), 1896 (CO); ^{1}H NMR (CDCl$_3$, 300 MHz) δ 7.28 (d, J = 4.9 Hz, 1H), 7.34 (d, J = 4.9 Hz, 1H), 7.53 (d, J = 4.6 Hz, 1H), 7.70 (d, J = 4.6 Hz, 1H), 7.88−8.06 (m, 8H), 8.12 (d, J = 7.9 Hz, 2H), 8.19 (d, J = 7.3 Hz, 2H), 8.31 (d, J = 7.6 Hz, 2H), 8.74−8.80 (m, 3H), 9.24 (s, 1H), 9.28 (d, J = 5.2 Hz, 1H); ^{13}C NMR (CDCl$_3$, 75 MHz) δ 111.05, 111.49, 118.79, 121.47, 122.30, 122.33, 122.35, 122.42, 123.93, 124.57, 124.62, 124.68, 124.74, 125.56, 125.61, 125.66, 125.71, 125.90, 125.93, 125.96, 126.02, 126.24, 126.80, 126.85, 126.90, 126.95, 127.69, 127.83, 128.79, 129.48, 129.99, 130.43, 130.52, 130.69, 130.74, 130.95, 131.12, 131.17, 131.58, 131.87, 132.02, 132.47, 133.10, 136.33, 137.06, 137.96, 137.98, 138.57, 140.94, 140.96, 141.47, 141.49, 143.40, 147.91, 147.93, 149.89, 153.65, 153.89, 153.94, 157.12, 162.68, 192.55, 192.98, 193.34 (Because the spectrum showed a complicated pattern due to C−F couplings, only distinctive peaks were listed.); MS (MALDI, positive) 1068.1 ([M−3(CO)]$^+$); UV−vis (CH$_2$Cl$_2$, λ_{max}/nm) 353, 494, 847, 944.

Preparation of 4i (3,5-Bis-trifluoromethylphenyl). Reaction temperature: 160 °C, reaction time: 21 h, 29% yield. IR (powder, cm^{-1}) 2009 (CO), 1913 (CO), 1899 (CO); ^{1}H NMR (CDCl$_3$, 300 MHz) δ 7.27 (d, J = 4.8 Hz, 1H), 7.29 (d, J = 4.8 Hz, 1H), 7.52 (d, J = 4.8 Hz, 1H), 7.67 (d, J = 4.8 Hz, 1H), 8.09 (s, 1H), 8.21 (s, 1H), 8.27 (br, m, 2H), 8.36 (s, 1H), 8.40 (s, 1H), 8.47 (br, m, 2H), 8.64 (s, 2H), 8.71 (d, J = 5.1 Hz, 1H), 9.06 (s, 2H), 9.25 (s, 1H), 9.39 (d, J = 5.1 Hz, 1H); ^{13}C NMR (CDCl$_3$, 75 MHz) δ 110.17, 110.77, 117.49, 121.28, 121.36, 121.41, 121.97, 122.05, 122.92, 122.96, 123.87, 124.40, 124.89, 124.98, 125.02, 126.80, 127.37, 127.81, 128.72, 128.81, 128.93, 129.17, 130.15, 130.18, 130.80, 130.95, 131.09, 131.19, 131.25, 131.69, 131.87, 132.02, 132.14, 132.27, 132.32, 132.76, 132.93, 133.21, 133.37, 133.82, 134.26, 134.52, 136.29, 136.73, 137.26, 139.12, 139.71, 143.60, 145.99, 149.85, 153.96, 154.14, 154.28, 156.73, 162.19, 191.76, 192.35, 192.98 (Because the spectrum showed complicated pattern due to C−F couplings, only distinctive peaks were listed.); MS (MALDI, positive) m/z = 1340.1 ([M−3(CO)]$^+$), 1368.1 ([M−2(CO)]$^+$), 1424.1 ([M]$^+$); UV−vis (CH$_2$Cl$_2$, λ_{max}/nm) 351, 494, 847, 943.

Preparation of 4j (4-Nitrophenyl). Reaction temperature: 130 °C, reaction time: 18 h, 28% yield. IR (powder, cm^{-1}) 2009 (CO), 1917 (CO), 1900 (CO), 1883 (CO); ^{1}H NMR (CDCl$_3$, 300 MHz) δ 7.30 (d, J = 4.5 Hz, 1H), 7.34 (d, J = 4.8 Hz, 1H), 7.54 (d, J = 4.5 Hz, 1H), 7.67 (d, J = 4.8 Hz, 1H), 8.02 (m, 2H), 8.24 (br, d, J = 8.4 Hz, 2H), 8.35 (d, J = 8.7 Hz, 2H), 8.53 (d, J = 8.4 Hz, 2H), 8.64 (m, 4H), 8.73 (d, J = 8.7 Hz, 2H), 8.77 (d, J = 5.1 Hz, 1H), 8.82 (d, J = 9.0 Hz, 2H), 9.23 (s, 1H), 9.35 (d, J = 5.1 Hz, 1H); ^{13}C NMR (It was, so far, difficult to measure the ^{13}C NMR of **4j** because of its low solubility in common deutrated organic solvents.); MS (MALDI, positive) m/z = 976.2 ([M−3(CO)]$^+$); UV−vis (CH$_2$Cl$_2$, λ_{max}/nm) 351, 507, 511, 845, 942.

Reactions of NFTPP derivatives with Re$_2$(CO)$_{10}$. Reaction with NFTPP (7). A solution of **7** (6.2 mg, 10 μmol, 1.0 equiv) and Re$_2$(CO)$_{10}$ (3.5 mg, 5.4 μmol, 0.53 equiv) in 1,2-dichlorobenzene (6.0 mL) was degassed under reduced pressure (~0.3 mmHg) at 0 °C. The resulting mixture was heated at 130 °C for 41 h under

an argon atmosphere. After cooling, 1,2-dichlorobenzene was removed under reduced pressure, and the residue was purified by silica gel chromatography (eluent: CH_2Cl_2/hexane = 1:1). The first violet fraction collected was concentrated to dryness to give **4a** in 77% yield (6.9 mg, 7.8 μmol).

Reaction with 21-Br−NFTPP (6). A solution of **6** (20 mg, 29 μmol, 1.0 equiv) and $Re_2(CO)_{10}$ (21 mg, 32 μmol, 1.1 equiv) in chlorobenzene (20 mL) was heated at 130 °C for 16 h. After evaporation, the residue was subjected to silica gel column separation to give **4a** in 63% yield (16 mg, 18 μmol).

Synthesis of Re(NCTPP)(CO)$_3$ (8). Preparation of *N*-SEM-NCTPP (9). SEMCl (1.0 mL) was added to a solution of NCTPP in CH_2Cl_2, and the mixture was stirred at 27 °C for 1 d. After quenching with MeOH (10 mL) and Et_3N (5 mL), the resulting mixture was evaporated to dryness. The residue was purified with an alumina column (eluent: CH_2Cl_2), and then with a silica gel column (eluent: CH_2Cl_2/MeOH = 99:1). The second green band was collected, evaporated, and dried under reduced pressure to give **9** (500 mg, 83% yield) as a green solid. ^{1}H NMR ($CDCl_3$, 300 MHz) δ −0.21 (s, 9H), 0.57 (t, J = 8.2 Hz, 2H), 1.68 (d, J = 1.8 Hz, 1H), 2.96 (t, J = 8.2 Hz, 2H), 4.06 (br s, 1H), 4.92 (s, 2H), 7.41 (d, J = 4.6 Hz, 1H), 7.45 (d, J = 4.9 Hz, 1H), 7.48 (d, J = 1.8 Hz, 1H), 7.54−7.65 (m, 12H), 7.66 (d, J = 5.5 Hz, 1H), 7.69 (d, J = 5.5 Hz, 1H), 7.76 (d, J = 4.6 Hz, 1H), 7.78−7.84 (m, 4H), 7.88 (d, J = 4.6 Hz, 1H), 7.90−7.95 (m, 4H); ^{13}C NMR ($CDCl_3$, 75 MHz) δ −1.56, 17.45, 66.34, 78.40, 107.12, 115.33, 115.67, 124.54, 126.73, 127.17, 127.22, 127.23, 127.49, 127.79, 128.33, 129.17, 129.39, 130.52, 130.87, 130.98, 133.33, 133.51, 133.53, 134.56, 134.68, 134.84, 134.92, 135.02, 136.42, 136.87, 140.33, 141.13, 141.52, 141.56, 143.45, 143.79, 153.95, 154.77, 163.46, 163.81; MS (MALDI, positive) m/z = 744.5 ([M]$^+$).

Preparation of Re(*N*-SEM-NCTPP)(CO)$_3$ (10). A mixture of **9** (4.8 mg, 6.4 μmol, 1.0 equiv), $Re_2(CO)_{10}$ (5.1 mg, 7.8 μmol, 1.2 equiv), and Et_3N (10 μL) in 2.5 mL of PhCl was heated at 130 °C for 15 h. The reaction mixture was evaporated to dryness, and the residue was subjected to silica gel column chromatography (eluent: CH_2Cl_2/hexane = 1:4∼1:1) to give **10** in 48% yield (3.1 mg, 3.1 μmol) as a brown solid. IR (powder, cm^{-1}) 2007 (CO), 1905 (CO), 1865 (CO); ^{1}H NMR ($CDCl_3$, 300 MHz) δ −0.41 (d, J = 1.5 Hz, 1H), −0.08 (s, 9H), 0.75−0.82 (m, 2H), 3.22−3.32 (m, 2H), 4.79 (d, J = 9.9 Hz, 1H), 5.17 (d, J = 9.9 Hz, 1H), 7.24 (d, J = 1.5 Hz, 1H), 7.60−7.62 (m, 6H), 7.63−7.80 (m, 6H), 7.83 (d, J = 4.9 Hz, 1H), 7.86−7.93 (m, 7H), 8.00 (d, J = 4.9 Hz, 1H), 8.00−8.15 (m, 4H), 8.26 (d, J = 5.2 Hz, 1H); ^{13}C NMR ($CDCl_3$, 75 MHz) δ −1.51, 17.86, 67.48, 78.56, 101.65, 121.50, 122.35, 123.75, 125.78, 127.16, 127.17, 127.21, 127.41, 127.42, 127.85, 127.87, 128.49, 128.63, 128.80, 130.76, 130.97, 131.66, 131.82, 133.20, 135.64, 136.58, 136.89, 140.68, 141.68, 141.74, 153.79, 154.60, 156.80, 158.59, 163.61, 164.02, 190.98, 191.67, 192.73; MS (MALDI, negative) m/z = 1012.1 ([M]$^-$).

Preparation of Re(NCTPP)(CO)$_3$ (8). Tetrabutylammonium fluoride (1 M in THF, 100 μL) was added to a suspension of **10** (10 mg, 10 μmol) and MS3A (powder, 200 mg) in DMF (2.0 mL) at 26 °C, and the mixture was stirred at that temperature for 22 h. The resulting slurry was filtered, and the filtrate was washed with H_2O two times. The organic layer was dried over anhydrous Na_2SO_4, filtered, and evaporated to dryness. The residue was purified by silica gel column chromatography to give **8** in 30% yield (2.6 mg, 2.9 μmol). IR (powder, cm^{-1}) 2010 (CO), 1886 (CO); ^{1}H NMR ($CDCl_3$, 300 MHz) δ −0.45 (br s, 1H), 7.48 (d, J = 1.5 Hz, 1H), 7.60−7.64 (m, 6H), 7.64−7.83 (m, 6H), 7.91−7.98 (m, 5H), 8.00−8.15 (m, 5H), 8.20 (d, J = 7.0 Hz, 1H), 8.27 (d, J = 4.9 Hz, 1H), 8.38 (d, J = 4.9 Hz, 1H), 9.41 (br s, 1H); ^{13}C NMR ($CDCl_3$, 75 MHz) δ 105.34, 122.13, 122.29, 125.02, 126.35, 127.12, 127.16, 127.44, 127.46, 127.87, 127.93, 127.99, 128.34, 128.88, 130.96, 131.35, 131.49, 131.94, 133.30, 133.66, 134.91, 135.62, 136.67, 137.04, 138.20, 140.68, 141.71, 141.87, 153.54, 154.17, 157.13, 157.95, 162.90, 163.36, 190.36, 191.35, 192.29; MS (MALDI, negative) m/z = 881.1 ([M−H]$^-$).

Chemical Functionalization of 4a. Preparation of Re(21-NO$_2$−NFTPP)(CO)$_3$ (15). Sodium nitrite (500 mg) was dissolved in 50 mL of aqueous HCl solution (3.3 wt %), and the mixture was added to a CH_2Cl_2 (50 mL) solution of **4a** (200 mg). The resulting suspension was vigorously stirred at 25 °C for 5 min. After neutralization with Na_2CO_3, the organic layer was separated, dried over Na_2SO_4, and evaporated to dryness. The residue was subjected to silica gel column chromatography (eluted with CH_2Cl_2). The first reddish-purple band was collected and recrystallized with CH_2Cl_2/hexane to give 201 mg of **15** (95% yield). IR (powder, cm^{-1}) 2001 (CO), 1912 (CO), 1902 (CO), 1880 (CO); ^{1}H NMR ($CDCl_3$, 300 MHz) δ 7.42 (d, J = 4.8 Hz, 1H), 7.56 (d, J = 4.8 Hz, 1H), 7.70 (m, 15H), 7.87 (br, m, 2H), 8.01 (d, J = 5.1 Hz, 1H), 8.08 (br, d, J = 7.5 Hz, 2H), 8.19 (d, J = 7.2 Hz, 2H), 8.98 (d, J = 4.9 Hz, 1H), 9.19 (d, J = 4.9 Hz, 1H); ^{13}C NMR ($CDCl_3$, 75 MHz) δ 114.43, 120.19, 122.03, 122.12, 124.79, 127.48, 127.66, 128.10, 128.74, 128.80, 128.95, 129.10, 129.45, 129.79, 130.42, 131.94, 132.43, 132.61, 133.45, 133.60, 137.21, 137.54, 137.62, 138.10, 139.32, 139.73, 144.43, 146.03, 153.38, 155.80, 156.35, 156.75, 163.22, 191.16, 191.53, 192.78; MS (MALDI) m/z = 840.9 ([M−3CO]$^+$), 868.9 ([M−2CO]$^+$), 925.0 ([M]$^+$); UV−vis (CH_2Cl_2, λ_{max}/nm) 360, 539, 768, 860.

Preparation of Re(21-CHO−NFTPP)(CO)$_3$ (16). A solution of **4a** (30 mg, 0.034 mmol) in dichloromethane (15 mL) was added dropwise over 10 min to a solution of Vilsmeier−Haak reagent prepared from DMF (3.0 mL, 42 mmol) and phosphorus oxychloride (1.6 mL, 18 mmol). The resulting solution was stirred at 20 °C for 1 h and then neutralized with aqueous $NaHCO_3$ solution. The organic layer was separated, washed with water, and dried over Na_2SO_4. After evaporation, the residue was purified by silica gel column chromatography with CH_2Cl_2. The first purple fraction gave **16** (21 mg, 0.023 mmol) in 67% yield. IR (powder, cm^{-1}) 2004 (CO), 1907 (CO), 1888 (CO), 1880 (CO), 1647 (CHO); ^{1}H NMR ($CDCl_3$, 300 MHz) δ 7.51 (d, J = 4.8 Hz, 1H), 7.72 (m, 16H), 7.91 (br, m, 2H), 8.01 (d, J = 4.8 Hz, 1H), 8.09 (br, m, 2H), 8.24 (br, d, 2H), 9.01 (d, J = 5.1 Hz, 1H), 9.21 (d, J = 5.1 Hz, 1H), 10.07 (s, 1H); ^{13}C NMR ($CDCl_3$, 75 MHz) δ 117.45, 121.52, 121.74, 121.99, 124.79, 125.51, 127.39, 127.54, 127.61, 128.29, 128.48, 128.60, 128.63, 129.33, 129.81, 131.49, 133.34, 133.38, 133.51, 133.69, 136.70, 137.71, 137.86, 138.21, 138.40, 144.68, 146.98, 149.87, 155.78, 156.20, 156.30, 162.52, 186.09, 191.57, 192.24, 192.93; MS (MALDI) m/z = 823.7 ([M−3CO]$^+$), 851.7 ([M−2CO]$^+$); UV−vis (CH_2Cl_2, λ_{max}/nm) 353, 507, 533, 801, 892.

Preparation of Re(21-PhCO−NFTPP)(CO)$_3$ (17). To a solution of **4a** (20 mg, 0.027 mmol) in CH_2Cl_2 (10 mL) was added C_6H_5COCl (13 μL, 0.11 mmol, 5 equiv) and $AlCl_3$ (15 mg, 0.11 mmol, 5 equiv). After stirring at 24 °C for 3 h, the resulting mixture was washed with water and dried over Na_2SO_4. After evaporation, the residue was purified by silica gel column chromatography (eluent: CH_2Cl_2/hexane = 3:1). The first fraction gave unreacted **4a** (6.2 mg, 7.0 μmol, 24%), and the second fraction afforded **17** (7.3 mg, 7.4 μmol, 32%). IR (powder, cm^{-1}) 2002 (CO), 1904 (CO), 1890 (CO), 1656 (PhCO); ^{1}H NMR ($CDCl_3$, 300 MHz) δ 7.17 (d, J = 4.5 Hz, 2H), 7.22 (d, J = 7.8 Hz, 2H), 7.28 (2H), 7.43 (m, 3H), 7.51 (d, J = 4.8 Hz, 2H), 7.53 (s, 1H), 7.63 (m, 8H), 7.77 (br, m, 3H), 7.84 (br, m, 1H), 7.90 (d, J = 4.8 Hz, 2H), 8.09 (br, m, 1H), 8.19 (d, J = 7.2 Hz, 2H), 8.87 (d, J = 5.4 Hz, 1H), 9.15

(d, $J = 5.4$ Hz, 1H); ^{13}C NMR ($CDCl_3$, 75 MHz) δ 114.80, 120.12, 121.55, 122.90, 124.50, 127.41, 127.52, 127.58, 127.73, 127.79, 128.34, 128.39, 128.51, 128.96, 129.00, 129.20, 130.22, 131.70, 131.94, 132.31, 132.46, 133.22, 133.32, 137.19, 137.40, 137.56, 138.04, 140.31, 140.50, 144.92, 145.07, 146.95, 154.54, 154.60, 155.16, 155.96, 163.38, 192.35, 192.52, 193.31, 193.42; MS (MALDI) $m/z = 899.8$ ([M−3(CO)]$^+$), 927.8 ([M−2(CO)]$^+$); UV−vis (CH_2Cl_2, λ_{max}/nm) 358, 500, 533, 841, 922.

Preparation of Re(21-CN−NFTPP)(CO)$_3$ (19). To a CH_2Cl_2 solution of **4a** (30 mg, 0.034 mmol, 1.0 equiv) was added NBS (6.6 mg, 0.037 mmol, 1.1 equiv), and the resulting solution was stirred for 5 min. After evaporation, the residue was passed through a pad of silica gel. The purple filtrate was evaporated to give a crude product containing **18** as a major component. ^{1}H NMR ($CDCl_3$, 300 MHz) δ 7.25 (1H, overlapped with a signal due to $CHCl_3$), 7.31 (d, $J = 4.7$ Hz, 1H), 7.57−7.63 (m, 6H), 7.66−7.75 (m, 10H), 7.80−7.88 (m, 2H), 7.96−8.04 (m, 2H), 8.44 (d, $J = 7.9$ Hz, 2H), 8.72 (d, $J = 5.2$ Hz, 1H), 9.02 (d, $J = 5.2$ Hz, 1H); MS (MALDI, positive) $m/z = 873.7$ ([M−3(CO)]$^+$); UV−vis (CH_2Cl_2, λ_{max}/nm) 357, 493, 528, 650, 871, 964.

To a DMF solution of the crude product containing **18**, CuCN (8.0 mg, 0.089 mmol) was added, and the resulting mixture was heated at 150 °C for 3 h. After evaporation, the residue was purified by a silica gel column chromatography with CH_2Cl_2/hexane = 7:3. The first fraction gave the recovered **4a**, and the second fraction gave **19** in 53% yield (16.7 mg, 0.018 mmol). IR (powder, cm^{-1}) 2207 (CN), 2001 (CO), 1905 (CO), 1894 (CO); ^{1}H NMR ($CDCl_3$, 300 MHz) δ 7.47 (d, $J = 4.8$ Hz, 1H), 7.58 (d, $J = 4.8$ Hz, 1H), 7.63 (m, 4H), 7.81 (m, 10H), 7.91 (d, $J = 4.8$ Hz, 1H), 7.97 (d, $J = 4.8$ Hz, 1H), 8.03 (m, 4H), 8.65 (d, $J = 7.2$ Hz, 2H), 8.97 (d, $J = 4.8$ Hz, 1H), 9.31 (d, $J = 5.4$ Hz, 1H); ^{13}C NMR ($CDCl_3$, 75 MHz) δ 89.73, 114.68, 115.95, 121.52, 122.13, 124.18, 127.50, 127.51, 127.60, 127.67, 128.16, 128.66, 128.72, 129.06, 129.50, 129.84, 130.08, 131.31, 131.63, 132.18, 133.06, 133.33, 135.63, 137.26, 137.56, 137.66, 139.22, 143.96, 144.40, 149.62, 154.58, 154.87, 155.83, 156.88, 163.30, 191.77, 192.19, 192.94; MS (MALDI, positive) $m/z = 820.6$ ([M−3(CO)]$^+$), 848.6 ([M−2(CO)]$^+$); UV−vis (CH_2Cl_2, λ_{max}/nm): 361, 502, 770, 910.

Calculation Details. All of the DFT calculations were performed with the *Gaussian 03* program package[26] without symmetry assumption. The geometries were fully optimized at the Becke's three-parameter hybrid functional[27] combined with the Lee−Yang−Parr correlation functional[28] abbreviated as the B3LYP level of density functional theory. The LANL2DZ basis set[29] was used for rhenium and the 6-31G** basis sets for carbon, hydrogen, nitrogen, and oxygen. This combination was denoted as 631LAN.

Table 4. Crystal Data and Structure Analysis Results for Complexes **4a** and **15**

	4a·CH_2Cl_2	**15**·0.5CH_2Cl_2
formula	$C_{48}H_{29}Cl_2N_4O_3Re$	$C_{47.5}H_{27}ClN_5O_5Re$
cryst syst	monoclinic	monoclinic
space group	$P2_1/c$ (No. 14)	$C2/c$ (No. 15)
R	0.042	0.029
wR2 (all data)	0.043	0.062
GOF	1.155	0.928
a (Å)	14.8862(8)	37.386(2)
b (Å)	12.5444(7)	9.4452(5)
c (Å)	21.0094(12)	23.9734(12)
α (deg)	90	90
β (deg)	101.927(1)	115.175(1)
γ (deg)	90	90
V (Å^3)	3838.6(4)	7661.2(7)
Z	4	8
T (K)	90(2)	223(2)
cryst size (mm^3)	0.16 × 0.13 × 0.05	0.15 × 0.13 × 0.07
D_{calcd} (g cm^{-3})	1.673	1.681
$2\theta_{min}$, $2\theta_{max}$ (deg)	6.0, 55.8	3.5, 51.0
No. of rflns measd (unique)	9137	7135
No. of rflns measd ($I > 2\sigma(I)$)	6663	5759
No. of params	552	553
Δ (e Å^{-3})	2.36, −3.41	1.71, −0.80

X-ray Diffraction Studies. X-ray analysis was performed on a SMART APEX equipped with CCD detector (Brucker) using Mo Kα (graphite monochromated, $\lambda = 0.71069$ Å) radiation. Crystal data and data statistics for **4a** and **15** are summarized in Table 4. The structure of **4a** was solved by the direct method of *SIR-97*[30] and expanded using Fourier techniques of *DIRDIF-99*[31] using the crystal structure program package. The non-hydrogen atoms were refined anisotropically by the full-matrix least-square method. Hydrogen atoms were placed at calculated positions. The structure of **15** was solved by the direct method of *SHELXS-97* and refined using the *SHELXL-97* program.[32] The non-hydrogen atoms were refined anisotropically by the full-matrix least-square method. The hydrogen atoms were placed at calculated positions.

Acknowledgment. This research was supported by the Grant-in-Aid for Scientific Research (16350024) from Monbukagaku-sho, Japan, and PRESTO from JST, Japan.

Supporting Information Available: Cartesian coordinates for the optimized structures for **4a**, **8**, **A**, and **B**. This material is available free of charge via the Internet at http://pubs.acs.org. Crystallographic data for the structures reported in this article have been deposited with the Cambridge Crystallographic Data Centre as supplementary publication numbers CCDC 236715 (**4a**) and CCDC 649140 (**15**).

IC701208G

(26) Frisch, M. J.; Trucks, G. W.; Schlegel, H. B.; Scuseria, G. E.; Robb, M. A.; Cheeseman, J. R.; Montgomery, J. A., Jr.; Vreven, T.; Kudin, K. N.; Burant, J. C.; Millam, J. M.; Iyengar, S. S.; Tomasi, J.; Barone, V.; Mennucci, B.; Cossi, M.; Scalmani, G.; Rega, N.; Petersson, G. A.; Nakatsuji, H.; Hada, M.; Ehara, M.; Toyota, K.; Fukuda, R.; Hasegawa, J.; Ishida, M.; Nakajima, T.; Honda, Y.; Kitao, O.; Nakai, H.; Klene, M.; Li, X.; Knox, J. E.; Hratchian, H. P.; Cross, J. B.; Bakken, V.; Adamo, C.; Jaramillo, J.; Gomperts, R.; Stratmann, R. E.; Yazyev, O.; Austin, A. J.; Cammi, R.; Pomelli, C.; Ochterski, J. W.; Ayala, P. Y.; Morokuma, K.; Voth, G. A.; Salvador, P.; Dannenberg, J. J.; Zakrzewski, V. G.; Dapprich, S.; Daniels, A. D.; Strain, M. C.; Farkas, O.; Malick, D. K.; Rabuck, A. D.; Raghavachari, K.; Foresman, J. B.; Ortiz, J. V.; Cui, Q.; Baboul, A. G.; Clifford, S.; Cioslowski, J.; Stefanov, B. B.; Liu, G.; Liashenko, A.; Piskorz, P.; Komaromi, I.; Martin, R. L.; Fox, D. J.; Keith, T.; Al-Laham, M. A.; Peng, C. Y.; Nanayakkara, A.; Challacombe, M.; Gill, P. M. W.; Johnson, B.; Chen, W.; Wong, M. W.; Gonzalez, C.; Pople, J. A. *Gaussian 03*, revision C.02; Gaussian, Inc.: Wallingford, CT, 2004.
(27) Becke, A. D. *J. Chem. Phys.* **1993**, *98*, 5648.
(28) Lee, C.; Yang, W.; Parr, R. G. *Phys. Rev. B* **1988**, *37*, 785.
(29) Hay, P. J.; Wadt, W. R. *J. Chem. Phys.* **1985**, *82*, 270.
(30) Altomare, A.; Burla, M. C.; Camalli, G.; Cascarano, G.; Giacovazzo, C.; Guagliardi, Moliteri, A.; Polidori, G.; Rizzi, R. *J. Appl. Crystallogr.* **1999**, *32*, 115.
(31) Beurskens, P. T.; Beurskens, G.; de Gelder, R.; Garcia-Granda, S.; Gould, R. O.; Israel, R.; Smits, J. M. M. *The DIRDIF-99 program system*; Crystallography Laboratory: University of Nijmegen, The Netherlands, 1999.
(32) Sheldrick, G. M. *Program for the Solution of Crystal Structures*; University of Göttingen: Göttingen, Germany, 1997.